

Giant nonlinear conductivity in 2D electron gas from substrate-induced dipolar scattering

Dmitry V. Chichinadze,^{1,*} Alexander Seidel,¹ and Zohar Nussinov¹

¹*Department of Physics, Washington University in St. Louis, St. Louis, MO, 63130 USA*

Despite a surge of interest in the nonlinear transport in 2D materials, a fundamental puzzle remains: existing theoretical frameworks are unable to quantitatively account for the giant nonlinear conductivities ($\gtrsim 1 \frac{\mu\text{m}}{\Omega\text{V}}$) recently reported in 2D van der Waals heterostructures. Here, we introduce a mechanism based on electron scattering from a substrate-induced periodic dipole array. We show that the strict kinematic constraints, inherent to 2D scattering, lead to a singular enhancement of the nonlinear response, fundamentally dictating a natural scale of $1 \frac{\mu\text{m}}{\Omega\text{V}}$.

Introduction. In recent years, second order nonlinear electron transport in 2D systems with broken inversion symmetry has become a focus of intense research due to new physical effects and potential practical applications [1–15]. In this transport regime, Ohm’s law acquires quadratic corrections and, in component form, reads

$$j_i = \sigma_{ij} E_j + \tilde{\sigma}_{ijk} E_j E_k, \quad (1)$$

where σ_{ij} is a rank-2 linear conductivity tensor and $\tilde{\sigma}_{ijk}$ is a rank-3 nonlinear conductivity tensor. In the DC limit, which we consider in this work, $\tilde{\sigma}_{ijk}$ is symmetric under the interchange $j \leftrightarrow k$.

A central and pressing mystery is the origin of the giant second order nonlinear conductivity in 2D metallic systems, as highlighted in, e.g., [16, 17]. In these works, the nonlinear conductivity tensor extracted from experimental data was found to be orders of magnitude larger than theoretical estimates based on any known mechanism. This massive quantitative discrepancy is not merely a numerical detail; it signals a fundamental breakdown in our current understanding of nonlinear transport in 2D materials.

While several candidates have been proposed to bridge this gap, such as quantum corrections to conductivity (which are known to cause nonlinearities in the $I - V$ characteristics of low-dimensional systems [18, 19]) in transition metal dichalcogenide van der Waals (vdW) heterostructures [20] and complex electron-electron interaction effects [5], none have yet provided a universal or quantitatively consistent explanation for the observed scales. In this work, we provide a scenario that resolves the puzzle. We show that the scattering of conduction electrons off a periodic dipole array, inherent to ferroelectric substrates, generates nonlinear conductivity with a natural scale that matches experimental values. Although nonlinear transport in polar media has a rich history in 3D systems [21–24], we show that in 2D unique scattering anomalies elevate nonlinear response to a giant effect.

The experimental realization of such dipolar environments is common in 2D vdW heterostructures with broken inversion symmetry, where ferroelectric or ferrielec-

tric phases are engineered via external electric displacement fields, interlayer twist angle, or the relative shift between the layers. For example, 2D conductors encapsulated by hBN (or other binary compounds) appear to display ferroelectric behavior, as was shown in recent experiments [25, 26] and suggested by DFT calculations [27]. In addition to mesoscopic dipole moments, twisted ferroelectric systems were proposed to exhibit electric polarization features similar to merons and anti-merons [28, 29]. Importantly, even in bulk ferroelectric systems with polarization vortex textures, the dipoles at surface boundaries exhibit *in-plane* orientation of dipoles [30–35]. This means that conduction electrons in the immediate proximity of a ferroelectric surface are subject to a robust electric dipole potential.

There is a mounting amount of experimental evidence pointing towards an intimate link between the emergence of large $\tilde{\sigma}$ and the existence of ferro- or ferrielectric behavior in 2D vdW heterostructures. In graphene based heterostructures, for instance, $\tilde{\sigma}$ is dramatically enhanced when graphene is encapsulated between hBN [16, 36]. This configuration is known for its ferroelectric behavior under certain conditions [25]. Similar nonlinear electronic response was observed in other setups and materials intimately linked to ferroelectricity of electron dipole moments present in the system [37].

In this work, we consider a 2D isotropic Fermi gas subject to two distinct scattering mechanisms: conventional short range impurity scattering and scattering from a static periodic array of electric dipoles originating from the ferroelectric substrate. First, by employing symmetry analysis, we show that to linear order in the dipole moment, the C_3 -symmetric contribution to the nonlinear conductivity tensor vanishes. Next, we utilize the Boltzmann equation approach [23, 38], calculate the T -matrix to linear order in the dipole moment, and solve for distribution functions spanning both linear and nonlinear regimes. Crucially, we obtain that the scattering matrix is enhanced for forward scattering, which leads to a logarithmic divergence of $\tilde{\sigma}$ for weak screening of the dipole potential. Similar enhancement of forward scattering was recently reported for 2D Fermi liquids [39–41]. In our model, however, the enhancement is much

more prominent in the nonlinear regime due to the special role of gradients of the distribution functions. Our analysis yields a characteristic scale of $\tilde{\sigma} \sim 1 \frac{\mu\text{m}}{\Omega\nu}$, providing a microscopic mechanism capable of explaining the giant nonlinear conductivity in 2D electron systems.

Symmetry analysis. The structure of $\tilde{\sigma}_{ijk}$ is determined by the symmetry of a 2D electron gas (2DEG) proximitized to a ferroelectric substrate. We consider a 2DEG situated in the xy -plane with the substrate dipoles \mathbf{d} oriented along a fixed, arbitrary axis in 3D. To permit a non-vanishing DC nonlinear response, the 2D inversion symmetry $(x, y) \rightarrow (-x, -y)$ must be broken. We decompose the coordinate and dipole vectors into in-plane and out-of-plane components: $\mathbf{r} = \mathbf{r}^\perp + \mathbf{r}^\parallel$ and $\mathbf{d} = \mathbf{d}^\perp + \mathbf{d}^\parallel$, where \parallel denotes components in the xy -plane and \perp indicates the z -component.

For electrons confined to the 2DEG, $\mathbf{r}^\perp = z\hat{z} = 0$. Under *in-plane* inversion, the components transform as $\mathbf{d}^\parallel \rightarrow -\mathbf{d}^\parallel$ and $\mathbf{d}^\perp \rightarrow \mathbf{d}^\perp$. Since $U^{dip} \propto \mathbf{r} \cdot \mathbf{d}$, the dipole field will not be experienced by the 2DEG electrons if $\mathbf{d} \uparrow \hat{z}$, hence, the linear σ_{ij} and nonlinear $\tilde{\sigma}_{ijk}$ conductivity tensor leading order expansions in \mathbf{d} read

$$\begin{aligned} \sigma_{ij} E_j &\simeq \sigma_{ij}(\mathbf{d} = 0) E_j + \beta_{ijkl}^{d^\parallel} E_j d_k^\parallel d_l^\parallel, \\ \tilde{\sigma}_{ijk} E_j E_k &\simeq \tilde{\sigma}_{ijk}(\mathbf{d} = 0) E_j E_k + \gamma_{ijkl}^{d^\parallel} E_j E_k d_l^\parallel. \end{aligned} \quad (2)$$

These expressions are consistent with [22]. We note that the linear conductivity acquires only a quadratic correction, whereas the nonlinear conductivity contribution starts from the linear order in \mathbf{d} .

The structure of \mathbf{d}^\parallel -induced nonlinear conductivity is further elucidated by a symmetry analysis of the nonlinear Ohm relations. In the complex representation, quadratic corrections to Ohm's law in 2D are expressed as [17]

$$\begin{aligned} j_x^{(2)} + ij_y^{(2)} &= \Xi_-^{(2)} (E_x - iE_y)^2 + \\ &+ \Xi_+^{(2)} (E_x + iE_y)^2 + \Xi_0^{(2)} (E_x^2 + E_y^2), \end{aligned}$$

where in-plane rotation follows $v_x \pm iv_y \rightarrow e^{\pm i\alpha} (v_x \pm iv_y)$. By applying an in-plane rotation to \mathbf{j} and \mathbf{E} vectors one can see that the $(E_x - iE_y)^2$ -term is invariant upon 120° rotation (3-fold symmetric), while the other two terms are invariant only upon 360° rotation. Adding an in-plane dipole moment $d_x + id_y$ up to the linear order in $|\mathbf{d}|$ leads to

$$\begin{aligned} j_x^{(2)} + ij_y^{(2)} &= \beta_+(d_x - id_y)(E_x + iE_y)^2 + \\ &+ \beta_0(d_x + id_y)(E_x^2 + E_y^2), \end{aligned} \quad (3)$$

where β_+, β_0 are two complex constants, see SI for details. Fully longitudinal nonlinear response is governed by a 2D vector \mathcal{B} which satisfies $\mathcal{B}_x + i\mathcal{B}_y = \Xi_+^{(2)*} + \Xi_0^{(2)}$, while nonlinear Hall response (fully transverse) is governed by a vector \mathcal{C} , whose components follow $i\mathcal{C}_x + \mathcal{C}_y =$

$\Xi_+^{(2)} - \Xi_0^{(2)*}$ [17]. For a circular Fermi surface (FS), without loss of generality, we can pick our reference frame such that $\mathbf{d} \uparrow \hat{x}$. Then, $d_y = 0$ and by M_y mirror symmetry (around the xz -plane) $\text{Im}(\Xi_+^{(2)}) = \text{Im}(\Xi_0^{(2)}) = 0$. It follows that $\mathcal{B} \perp \mathcal{C}$, satisfying

$$\mathcal{B}_y \equiv 0, \quad \mathcal{C}_x \equiv 0, \quad (4)$$

i.e., $\mathcal{B} \parallel \mathbf{d}$ and $\mathcal{C} \perp \mathbf{d}$. The signs of the nonzero components \mathcal{B}_x and \mathcal{C}_y are determined by the dispersion-specific constants β_+, β_0 . Therefore, for a circular FS in the presence of dipoles with moderate $|\mathbf{d}|$, the 3-fold rotationally symmetric contribution to $\tilde{\sigma}$ is vanishingly small, in contrast to the purely longitudinal \mathcal{B} and nonlinear Hall \mathcal{C} contributions.

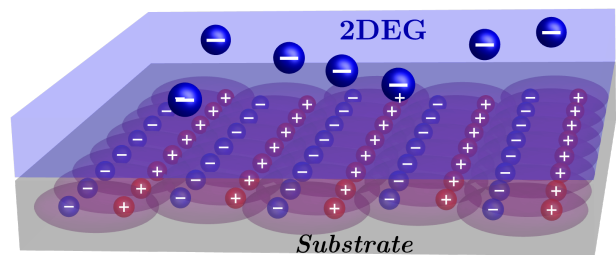


Figure 1. Schematic of the physical system. Electrons in a 2D gas (blue) scatter from an array of electric dipoles (purple) originating from the substrate (gray).

The model. We consider a 2D electron system coupled to a periodic array of point dipoles in the presence of a short-range disorder potential. Each point scatterer is treated as an individual dipole. The Fourier transform of the potential from a single dipole is

$$U^{dip}(\mathbf{k}) = \frac{-2\pi i \mathbf{e} \mathbf{d} \cdot \mathbf{k}}{\varepsilon k}, \quad (5)$$

where \mathbf{d} is the dipole moment of a single dipole, ε is the dielectric permittivity, and all dipoles are assumed to have the same moment and orientation. The short-range disorder from impurities is governed by $U^s(\mathbf{r}) = a \sum_{\mathbf{r}_i} \delta(\mathbf{r} - \mathbf{r}_i)$. The setup is analogous to that in [23, 24], except the system is two-dimensional and inversion is a 2D symmetry.

To calculate σ and $\tilde{\sigma}$, we employ the Boltzmann equation [38]

$$-\frac{e}{\hbar} \mathbf{E} \cdot \frac{\partial f(\mathbf{k})}{\partial \mathbf{k}} = - \int \frac{d^2 \mathbf{k}'}{(2\pi)^2} W_{\mathbf{k}\mathbf{k}'} (f(\mathbf{k}) - f(\mathbf{k}')), \quad (6)$$

where the scattering probability (matrix) $W_{\mathbf{k}\mathbf{k}'}$ satisfies

$$W_{\mathbf{k}\mathbf{k}'} = \frac{2\pi}{\hbar} |T_{\mathbf{k},\mathbf{k}'}|^2 \delta(\varepsilon_{\mathbf{k}} - \varepsilon_{\mathbf{k}'}), \quad (7)$$

with scattering being controlled by a T -matrix $T_{\mathbf{k},\mathbf{k}'}$. To study the effect of dipole scatterers on electron transport in the system we follow [23, 24] and calculate the T -matrix up to the leading term in \mathbf{d} ,

$$|T_{\mathbf{k},\mathbf{k}'}|^2 = n_{imp}a^2 + \frac{4n_{imp}a^2\pi^2e}{\varepsilon} \sum_{\mathbf{p}} \mathbf{d} \cdot \left[\frac{\mathbf{k} - \mathbf{k}'}{|\mathbf{k} - \mathbf{k}'|} - \frac{\mathbf{k} - \mathbf{p}}{|\mathbf{k} - \mathbf{p}|} - \frac{\mathbf{p} - \mathbf{k}'}{|\mathbf{p} - \mathbf{k}'|} \right] \delta(\omega - \varepsilon_{\mathbf{k}}) \Big|_{\omega=\varepsilon_{\mathbf{k}}}, \quad (8)$$

where n_{imp} is the impurity concentration.

We consider a 2D electron gas with dispersion $\varepsilon_{\mathbf{k}} = \frac{\hbar^2 \mathbf{k}^2}{2m} - \mu$, scattering off a periodic array of dipoles. For such a dispersion, the scattering probability $W_{\mathbf{k},\mathbf{k}'}$ can be evaluated explicitly:

$$W_{\mathbf{k},\mathbf{k}'} = \frac{2\pi n_{imp}}{\hbar} \left(a^2 + \frac{k_F a^2 e}{\hbar \varepsilon} \sqrt{\frac{m}{2\mu}} \mathbf{d} \cdot (\mathbf{k} - \mathbf{k}') \left[\frac{2\pi}{|\mathbf{k} - \mathbf{k}'|} - \frac{4}{k_F} \right] \right) \delta(\varepsilon_{\mathbf{k}} - \varepsilon_{\mathbf{k}'}). \quad (9)$$

We then introduce the standard parameterization for distribution functions at linear $f_1(\mathbf{k}) = \Phi_1(\mathbf{k}) \frac{\partial f_0(\varepsilon)}{\partial \varepsilon} \Big|_{\varepsilon=\varepsilon(\mathbf{k})}$ and quadratic $f_2(\mathbf{k}) = \Phi_{2,1}(\mathbf{k}) \frac{\partial f_0(\omega)}{\partial \omega} \Big|_{\omega=\varepsilon_{\mathbf{k}}} + \Phi_{2,2}(\mathbf{k}) \frac{\partial^2 f_0(\omega)}{\partial \omega^2} \Big|_{\omega=\varepsilon_{\mathbf{k}}}$ order in electric field, where $f_0(\varepsilon_{\mathbf{k}}) = n_F(\varepsilon_{\mathbf{k}})$ is the equilibrium distribution function at the Fermi surface. After such parameterization and introducing scattering rate $g(\mathbf{k}) = \int \frac{d^2 \mathbf{k}'}{(2\pi)^2} W_{\mathbf{k},\mathbf{k}'}$, the three equations that define linear and nonlinear electron transport properties are [17]

$$\begin{aligned} \Phi_1(\mathbf{k}) &= \frac{e}{\hbar} \frac{\mathbf{E}}{g(\mathbf{k})} \cdot \frac{\partial \varepsilon_{\mathbf{k}}}{\partial \mathbf{k}} + \int \frac{d^2 \mathbf{k}'}{(2\pi)^2} \frac{W_{\mathbf{k},\mathbf{k}'}}{g(\mathbf{k})} \Phi_1(\mathbf{k}'), \quad (10) \\ \Phi_{2,1}(\mathbf{k}) &= \frac{e\mathbf{E}}{\hbar g(\mathbf{k})} \cdot \frac{\partial \Phi_1(\mathbf{k})}{\partial \mathbf{k}} + \int \frac{d^2 \mathbf{k}'}{(2\pi)^2} \frac{W_{\mathbf{k},\mathbf{k}'}}{g(\mathbf{k})} \Phi_{2,1}(\mathbf{k}'), \\ \Phi_{2,2}(\mathbf{k}) &= \frac{e\mathbf{E} \cdot \frac{\partial \varepsilon(\mathbf{k})}{\partial \mathbf{k}}}{\hbar} \frac{\Phi_1(\mathbf{k})}{g(\mathbf{k})} + \int \frac{d^2 \mathbf{k}'}{(2\pi)^2} \frac{W_{\mathbf{k},\mathbf{k}'}}{g(\mathbf{k})} \Phi_{2,2}(\mathbf{k}') \end{aligned}$$

Solving for three Φ -functions allows then to calculate

$$\frac{\partial \Phi_1(\mathbf{k})}{\partial k_\alpha} = \frac{e}{\hbar} \frac{\partial}{\partial k_\alpha} \left(\frac{\mathbf{E} \cdot \frac{\partial \varepsilon(\mathbf{k})}{\partial \mathbf{k}}}{g(\mathbf{k})} \right) + \frac{2e}{\hbar \varepsilon} \sqrt{\frac{m}{2\mu}} \ln \left(\frac{\pi + \xi}{\xi} \right) [d_x \cos \theta + d_y \sin \theta] (\cos \theta, \sin \theta)_\alpha \sum_{n=1}^{\infty} (\Phi_1^{c,n} \cos n\theta + \Phi_1^{s,n} \sin n\theta),$$

where we have invoked the periodicity of $\Phi_1(\mathbf{k})$ on the FS via the expansion $\Phi_1(\theta) =$

electron current density using

$$\begin{aligned} j_\alpha &= -\frac{e}{\hbar} \int \frac{d^2 \mathbf{k}}{(2\pi)^2} \frac{\partial \varepsilon(\mathbf{k})}{\partial k_\alpha} \Phi_1(\mathbf{k}) \frac{\partial f_0(\varepsilon)}{\partial \varepsilon} \Big|_{\varepsilon=\varepsilon(\mathbf{k})} - \\ &= -\frac{e}{\hbar} \int \frac{d^2 \mathbf{k}}{(2\pi)^2} \left(\frac{\partial \varepsilon(\mathbf{k})}{\partial k_\alpha} \Phi_{2,1}(\mathbf{k}) - \frac{\partial \Phi_{2,2}(\mathbf{k})}{\partial k_\alpha} \right) \frac{\partial f_0(\omega)}{\partial \omega} \Big|_{\omega=\varepsilon_{\mathbf{k}}}. \quad (13) \end{aligned}$$

The role of gradients. Closed form analytical solutions for the functions Φ and the conductivities $\sigma, \tilde{\sigma}$ may be obtained within our model. We first examine the gradients of the distribution functions which enter the integral equations (11) and (12):

$$\begin{aligned} \frac{\partial \Phi_1(\mathbf{k})}{\partial k_\alpha} &= \frac{e}{\hbar} \frac{\partial}{\partial k_\alpha} \left(\frac{\mathbf{E} \cdot \frac{\partial \varepsilon(\mathbf{k})}{\partial \mathbf{k}}}{g(\mathbf{k})} \right) + \int \frac{d^2 \mathbf{k}'}{(2\pi)^2} \frac{\partial W_{\mathbf{k},\mathbf{k}'}}{\partial k_\alpha} \Phi_1(\mathbf{k}'), \\ \frac{\partial \Phi_{2,2}(\mathbf{k})}{\partial k_\alpha} &= \frac{\partial}{\partial k_\alpha} \left(\frac{eE_\beta \frac{\partial \varepsilon(\mathbf{k})}{\partial k_\beta}}{\hbar g(\mathbf{k})} \right) \Phi_1(\mathbf{k}) + \frac{eE_\beta \frac{\partial \varepsilon(\mathbf{k})}{\partial k_\beta}}{\hbar g(\mathbf{k})} \frac{\partial \Phi_1(\mathbf{k})}{\partial k_\alpha} + \\ &+ \frac{1}{g(\mathbf{k})} \int \frac{d^2 \mathbf{k}'}{(2\pi)^2} \frac{\partial W_{\mathbf{k},\mathbf{k}'}}{\partial k_\alpha} \Phi_{2,2}(\mathbf{k}'). \quad (14) \end{aligned}$$

The main contribution to the gradients of distribution functions comes from $\frac{\partial W_{\mathbf{k},\mathbf{k}'}}{\partial k_\alpha}$, which is given by

$$\frac{\partial W_{\mathbf{k},\mathbf{k}'}}{\partial \mathbf{k}} = \frac{2\pi n_{imp}}{\hbar} \frac{k_F a^2 e}{\hbar \varepsilon} \sqrt{\frac{m}{2\mu}} \left[\frac{2\pi \mathbf{d}_{\mathbf{k}-\mathbf{k}'}}{|\mathbf{k} - \mathbf{k}'|} - \frac{4\mathbf{d}}{k_F} \right] \delta(\varepsilon_{\mathbf{k}} - \varepsilon_{\mathbf{k}'}),$$

where

$$\mathbf{d}_{\mathbf{k}-\mathbf{k}'}^\perp = \mathbf{d} - \frac{\mathbf{k} - \mathbf{k}'}{|\mathbf{k} - \mathbf{k}'|} \left(\mathbf{d} \cdot \frac{\mathbf{k} - \mathbf{k}'}{|\mathbf{k} - \mathbf{k}'|} \right)$$

is orthogonal to $\mathbf{k} - \mathbf{k}'$. This contribution exhibits a logarithmic divergence, resulting in an enhancement of the nonlinear conductivity in the 2D system (see SI):

$\sum_{n=1}^{\infty} (\Phi_1^{c,n} \cos n\theta + \Phi_1^{s,n} \sin n\theta)$ and introduced the regularization parameter $\xi = k_{scr}/k_F$ with the dipole screening momentum k_{scr} . The enhancement is a consequence of kinematic constraints in 2D scattering, similar to the collinear scattering probability enhancement described in [39]. Notably, for the dipole array, the forward scattering probability *gradient* $\frac{\partial W_{\mathbf{k},\mathbf{k}'}}{\partial \mathbf{k}}$ exhibits a logarithmic divergence. This leads to a significant enhancement of the gradient terms, making the effect much more prominent in the nonlinear transport regime than in the linear one.

Solutions for distribution functions, σ , and $\tilde{\sigma}$. Performing Fourier decompositions of $\Phi_1(\mathbf{k})$, $\Phi_{2,1}(\mathbf{k})$ and $\Phi_{2,2}(\mathbf{k})$ one can analytically solve for *all* distribution functions and calculate σ , and $\tilde{\sigma}$. Introducing

$$\begin{aligned} \alpha &= \hbar^4 \frac{ek_F (E_x + iE_y)}{m^2 n_{imp} a^2}, & \beta &= \frac{k_F e}{\hbar \varepsilon} \sqrt{\frac{m}{2\mu}}, \\ \bar{d} &= d_x - id_y, & Z_n &= \Phi_1^{c,n} + i\Phi_1^{s,n}, \\ a_n &= \frac{-4(n+1) - 2}{4(n+1)^2 - 1}, & b_n &= \frac{4(n-1) - 2}{4(n-1)^2 - 1} \end{aligned} \quad (15)$$

one can cast the integral equation for $\Phi_1(\mathbf{k})$ into a compact algebraic form

$$Z_1 = \alpha + \beta a_1 \bar{d} Z_2, \quad (16)$$

$$Z_n = \beta a_n \bar{d} Z_{n+1} + \beta b_n d Z_{n-1}. \quad (17)$$

This may be solved recursively

$$\rho_n = \frac{Z_{n+1}}{Z_n}, \quad \rho_{n-1} = \frac{\beta b_n d}{1 - \beta a_n \bar{d} \rho_n}, \quad (18)$$

leading to a continued fraction representation for ρ_1 ,

$$\rho_1 = \frac{\beta b_2 d}{1 - \frac{\beta a_2 \bar{d} \beta b_3 d}{1 - \frac{\beta a_3 \bar{d} \beta b_4 d}{\dots}}}. \quad (19)$$

Eq. (19) can be evaluated numerically with arbitrary precision. Analogous closed-form expressions for $\Phi_{2,1}(\mathbf{k})$ and $\Phi_{2,2}(\mathbf{k})$ are presented in the SI. The continued fraction structure of the solutions is indicative of the coupling between different angular harmonics, resembling the results of [40, 41]. The distribution function solutions allow for a direct evaluation of the linear

$$j_\gamma^{(1)} = \frac{e k_F}{\hbar 4\pi} \left(\text{Re} \left(\frac{\alpha}{1 - \beta a_1 \bar{d} \rho_1} \right), \text{Im} \left(\frac{\alpha}{1 - \beta a_1 \bar{d} \rho_1} \right) \right)_\gamma, \quad (20)$$

and nonlinear current density

$$\begin{aligned} j_\alpha^{(2)} &= \frac{\pi e k_F}{\hbar (2\pi)^2} \left(\Phi_{2,1}^{c,1}, \Phi_{2,1}^{s,1} \right)_\alpha - \frac{\pi m e^2}{\varepsilon \hbar^4 (2\pi)^2} \sqrt{\frac{m}{2\mu}} \ln \left(\frac{\pi + \xi}{\xi} \right) \left(d_x \Phi_{2,2}^{c,2} + d_y \Phi_{2,2}^{s,2}, d_x \Phi_{2,2}^{s,2} - d_y \Phi_{2,2}^{c,2} \right)_\alpha - \\ &- \frac{\pi e}{\hbar \varepsilon} \sqrt{\frac{m}{2\mu}} \ln \left(\frac{\pi + \xi}{\xi} \right) \frac{e^2 \hbar E_\beta k_F}{m n_{imp} a^2 (2\pi)^2} \left(\left(\frac{3d_x \Phi_1^{c,1}}{2} + \frac{d_y \Phi_1^{s,1}}{2} + \frac{d_x \Phi_1^{c,3}}{2} + \frac{d_y \Phi_1^{s,3}}{2} \right) \left(\frac{d_y \Phi_1^{c,1}}{2} + \frac{d_x \Phi_1^{s,1}}{2} - \frac{d_y \Phi_1^{c,3}}{2} + \frac{d_x \Phi_1^{s,3}}{2} \right) \right)_{\alpha\beta} \\ &\left(\frac{d_y \Phi_1^{c,1}}{2} + \frac{d_x \Phi_1^{s,1}}{2} - \frac{d_y \Phi_1^{c,3}}{2} + \frac{d_x \Phi_1^{s,3}}{2} \right) \left(\frac{d_x \Phi_1^{c,1}}{2} + \frac{3d_y \Phi_1^{s,1}}{2} - \frac{d_x \Phi_1^{c,3}}{2} - \frac{d_y \Phi_1^{s,3}}{2} \right) \right)_{\alpha\beta}. \end{aligned} \quad (21)$$

In Eq. (20), $\sigma \propto |\mathbf{d}|^2$ as ρ_1 is a function of d , which is in accordance with symmetry analysis, Eq. (2). Nonlinear conductivity $\tilde{\sigma}$, as is directly evident from Eq. (21), is logarithmically-divergent for small ξ , which enhances the magnitude of $\tilde{\sigma}$.

Scale of the nonlinear conductivity. Giant nonlinear conductivity has been reported in 2D materials with magnitudes ranging from $\sim 1 \frac{\mu\text{m}}{\Omega\text{V}}$ to $\sim 10^4 \frac{\mu\text{m}}{\Omega\text{V}}$ [16, 17, 36, 42]. To estimate the magnitude of the nonlinear conductivity in our model, we consider effective mass of charge carriers in units of electron mass m_e and fix the disorder strength and concentration of impurities by fixing the scattering time. For a single spinless band with $m = 0.5m_e$, $|\mathbf{d}| = 0.5e\text{\AA}$, $\tau = 10^{-11} \text{s}$ we obtain $\tilde{\sigma} \sim 1 \frac{\mu\text{m}}{\Omega\text{V}}$, which defines the natural scale for nonlinear conductivity arising from dipole scattering in a 2DEG, see Fig. 2. The dependence on the screening length is logarithmic,

and for these parameters, the linear conductivity is $\sigma \sim 20 \frac{e^2}{\hbar}$, which is well within the realistic range. In contrast to other proposed mechanisms, the enhancement here is a consequence of the physical scattering anomaly, which fundamentally dictates the $\frac{\mu\text{m}}{\Omega\text{V}}$ scale independently of specific parameter tuning.

Discussion and outlook. In summary, we have shown that the scattering of 2D electrons from an array of substrate dipoles provides a powerful and robust mechanism for generating giant nonlinear conductivity. Our theory naturally predicts a characteristic scale of $\tilde{\sigma} \sim 1 \frac{\mu\text{m}}{\Omega\text{V}}$, providing a quantitative resolution to recent experimental puzzles. We also find that to leading order in the dipole moment, the three-fold symmetric contribution to the nonlinear conductivity tensor vanishes – a result dictated by the symmetry of in-plane dipoles and resembling recent observations [17].

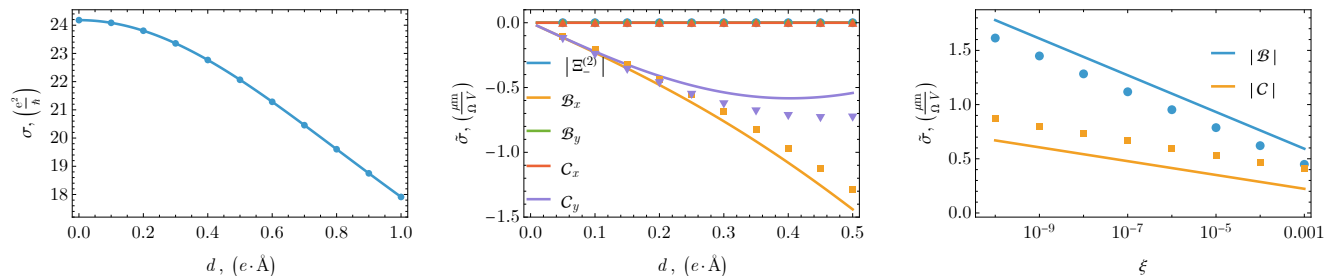


Figure 2. (Left) Linear conductivity as a function of dipole moment. (Middle) Components of the nonlinear conductivity tensor as a function of dipole moment, consistent with the symmetry analysis. (Right) Nonzero components of the nonlinear conductivity tensor as a function of ξ (log-linear plot). Solid lines indicate the analytical solution, while scatter points show numerical solution obtained using method of iterations with Direct Inversion in the Iterative Subspace (DIIS) to enforce convergence. The minor discrepancy in $\tilde{\sigma}$ is due to the logarithmic accuracy of the analytical solution. We used $m = 0.5m_e$, $\tau = 10^{-11}$ s, $\mu = 10^{-2}$ eV, with $d_y = 0$ for all panels; $\xi = 10^{-8}$ in the left and middle panels, and $|\mathbf{d}| = 0.5e\text{\AA}$ in the right panel.

The microscopic origin of this giant enhancement is a phenomenon specific to 2D, arising from the singular behavior of forward (collinear) scattering. While the setup is reminiscent of classic problems in polar materials [22–24], the crucial detail here is the 2D geometry, which imposes stricter kinematic constraints for scattering in Fermi liquids and gases [39]. Most importantly, this enhancement is an intrinsic feature of the nonlinear transport regime; it is driven by the scattering probability gradients, $\frac{\partial W_{\mathbf{k},\mathbf{k}'}}{\partial \mathbf{k}}$, which remain latent in the linear response but emerge as the dominant factor in *nonlinear* current generation.

Notably, this mechanism is quite general and not limited to dipole potentials. Higher order multipoles, such as octupoles, could yield even more singular enhancements of collinear scattering, potentially realizable in piezoelectric substrates [21, 37]. The net effect in such systems, however, will depend on a delicate interplay between stronger scattering singularities and typically smaller multipole moments, as large higher-order multipole moments are rather rare in condensed matter systems [43–46].

By bridging the gap between fundamental results in ferroelectric response theory [23] and 2D scattering anomalies [39], our work establishes a scenario for giant nonlinear conductivity generation. These results not only clarify the nature of nonreciprocal transport in 2D systems but also pave the way for engineering of nonlinear conductivity tensors through substrate control – a promising direction for 2D electronics and quantum device applications.

Acknowledgments. We thank E. Henriksen, A. Levchenko, JIA Li, R. Mishra, P. Sukhachov, O. Vafek for useful discussions. D.V.C. acknowledges financial support from Washington University in St. Louis through Edwin Thompson Jaynes Postdoctoral Fellowship.

* cdmity@wustl.edu

- [1] V. Genkin and P. Mednis, Contribution to the theory of nonlinear effects in crystals with account taken of partially filled bands, *Sov. Phys. JETP* **27**, 609 (1968).
- [2] S. Onoda, N. Sugimoto, and N. Nagaosa, Theory of non-equilibrium states driven by constant electromagnetic fields: Non-commutative quantum mechanics in the keldysh formalism, *Progress of Theoretical Physics* **116**, 61 (2006).
- [3] Y. Gao, S. A. Yang, and Q. Niu, Field induced positional shift of bloch electrons and its dynamical implications, *Phys. Rev. Lett.* **112**, 166601 (2014).
- [4] I. Sodemann and L. Fu, Quantum nonlinear hall effect induced by berry curvature dipole in time-reversal invariant materials, *Phys. Rev. Lett.* **115**, 216806 (2015).
- [5] T. Morimoto and N. Nagaosa, Nonreciprocal current from electron interactions in noncentrosymmetric crystals: roles of time reversal symmetry and dissipation, *Scientific Reports* **8**, 2973 (2018).
- [6] E. J. König, M. Dzero, A. Levchenko, and D. A. Pesin, Gyrotropic hall effect in berry-curved materials, *Phys. Rev. B* **99**, 155404 (2019).
- [7] H. Isobe, S.-Y. Xu, and L. Fu, High-frequency rectification via chiral bloch electrons, *Science Advances* **6**, eaay2497 (2020), <https://www.science.org/doi/pdf/10.1126/sciadv.aay2497>.
- [8] C. Wang, Y. Gao, and D. Xiao, Intrinsic nonlinear hall effect in antiferromagnetic tetragonal cumnans, *Phys. Rev. Lett.* **127**, 277201 (2021).
- [9] Z. Z. Du, C. M. Wang, H.-P. Sun, H.-Z. Lu, and X. C. Xie, Quantum theory of the nonlinear hall effect, *Nature Communications* **12**, 5038 (2021).
- [10] Z. Du, C.-H. Wang, H.-P. Sun, H.-Z. Lu, and X. C. Xie, Nonlinear Hall effects, *Nature Reviews Physics* **3**, 744 (2021).
- [11] C. Ortix, Nonlinear hall effect with time-reversal symmetry: Theory and material realizations, *Advanced Quantum Technologies* **4**, 2100056 (2021), <https://advanced.onlinelibrary.wiley.com/doi/pdf/10.1002/qute.2021>
- [12] F. Freimuth, S. Blügel, and Y. Mokrousov, Theory of unidirectional magnetoresistance and nonlinear hall ef-

- fect, *Journal of Physics: Condensed Matter* **34**, 055301 (2022).
- [13] K. Das, S. Lahiri, R. B. Atencia, D. Culcer, and A. Agarwal, Intrinsic nonlinear conductivities induced by the quantum metric, *Phys. Rev. B* **108**, L201405 (2023).
- [14] R. B. Atencia, D. Xiao, and D. Culcer, Disorder in the nonlinear anomalous hall effect of \mathcal{PT} -symmetric dirac fermions, *Phys. Rev. B* **108**, L201115 (2023).
- [15] M. Suárez-Rodríguez, F. De Juan, I. Souza, M. Gobbi, F. Casanova, and L. E. Hueso, Non-linear transport in non-centrosymmetric systems: From fundamentals to applications, *Nature Materials* **24**, 1005 (2025).
- [16] P. He, G. K. W. Koon, H. Isobe, J. Y. Tan, J. Hu, A. H. C. Neto, L. Fu, and H. Yang, Graphene moiré superlattices with giant quantum nonlinearity of chiral block electrons, *Nature Nanotechnology* **17**, 378 (2022).
- [17] D. V. Chichinadze, N. J. Zhang, J.-X. Lin, E. Morissette, X. Wang, K. Watanabe, T. Taniguchi, O. Vafek, and J. I. A. Li, Observation of giant nonlinear hall conductivity in bernal bilayer graphene (2025), arXiv:2411.11156 [cond-mat.mes-hall].
- [18] M. Leadbeater, R. Raimondi, P. Schwab, and C. Castellani, Non-linear conductivity and quantum interference in disordered metals, *The European Physical Journal B - Condensed Matter and Complex Systems* **15**, 277 (2000).
- [19] P. Schwab and R. Raimondi, Coherent transport in disordered metals out of equilibrium, *The European Physical Journal B - Condensed Matter and Complex Systems* **24**, 525 (2001).
- [20] D. V. Chichinadze, Weak localization and antilocalization corrections to nonlinear transport: a semiclassical boltzmann treatment (2025), arXiv:2510.02684 [cond-mat.mes-hall].
- [21] V. I. Belinicher and B. I. Sturman, The photogalvanic effect in media lacking a center of symmetry, *Soviet Physics Uspekhi* **23**, 199 (1980).
- [22] A. Gorbatshevich, Y. V. Kopaev, and V. Tugushev, Anomalous nonlinear effects at phase transitions to ferroelectric and magnetoelectric states, *Sov. Phys.-JETP* **58**, 643 (1983).
- [23] V. Belinicher, V. Malinovskii, and B. Sturman, Photogalvanic effect in a crystal with polar axis, *Soviet Journal of Experimental and Theoretical Physics* **46**, 362 (1977).
- [24] V. I. Belinicher and B. I. Sturman, The photogalvanic effect in media lacking a center of symmetry, *Soviet Physics Uspekhi* **23**, 199 (1980).
- [25] K. Yasuda, X. Wang, K. Watanabe, T. Taniguchi, and P. Jarillo-Herrero, Stacking-engineered ferroelectricity in bilayer boron nitride, *Science* **372**, 1458 (2021), <https://www.science.org/doi/pdf/10.1126/science.abd3230>.
- [26] L. Zhang, J. Ding, H. Xiang, N. Liu, W. Zhou, L. Wu, N. Xin, K. Watanabe, T. Taniguchi, and S. Xu, Electronic ferroelectricity in monolayer graphene moiré superlattices, *Nature Communications* **15**, 10905 (2024).
- [27] L. Li and M. Wu, Binary compound bilayer and multilayer with vertical polarizations: Two-dimensional ferroelectrics, multiferroics, and nanogenerators, *ACS Nano* **11**, 6382 (2017).
- [28] D. Bennett, G. Chaudhary, R.-J. Slager, E. Bousquet, and P. Ghosez, Polar meron-antimeron networks in strained and twisted bilayers, *Nature Communications* **14**, 1629 (2023).
- [29] D. Bennett, W. J. Jankowski, G. Chaudhary, E. Kaxiras, and R.-J. Slager, Theory of polarization textures in crystal supercells, *Phys. Rev. Res.* **5**, 033216 (2023).
- [30] I. I. Naumov, L. Bellaiche, and H. Fu, Unusual phase transitions in ferroelectric nanodisks and nanorods, *Nature* **432**, 737 (2004).
- [31] A. Yadav, C. Nelson, S. Hsu, Z. Hong, J. Clarkson, C. Schlepütz, A. Damodaran, P. Shafer, E. Arenholz, L. Dedon, *et al.*, Observation of polar vortices in oxide superlattices, *Nature* **530**, 198 (2016).
- [32] A. R. Damodaran, J. D. Clarkson, Z. Hong, H. Liu, A. K. Yadav, C. T. Nelson, S.-L. Hsu, M. R. McCarter, K.-D. Park, V. Kravtsov, A. Farhan, Y. Dong, Z. Cai, H. Zhou, P. Aguado-Puente, P. García-Fernández, J. Íñiguez, J. Junquera, A. Scholl, M. B. Raschke, L.-Q. Chen, D. D. Fong, R. Ramesh, and L. W. Martin, Phase coexistence and electric-field control of toroidal order in oxide superlattices, *Nature Materials* **16**, 1003 (2017).
- [33] P. Shafer, P. García-Fernández, P. Aguado-Puente, A. R. Damodaran, A. K. Yadav, C. T. Nelson, S.-L. Hsu, J. C. Wojdel, J. Íñiguez, L. W. Martin, E. Arenholz, J. Junquera, and R. Ramesh, Emergent chirality in the electric polarization texture of titanate superlattices, *Proceedings of the National Academy of Sciences* **115**, 915 (2018), <https://www.pnas.org/doi/pdf/10.1073/pnas.1711652115>.
- [34] B. Zhao, G. Y. Jung, S. Singh, R. B. Smith, H. Chen, G. Ren, C. Wang, S. Termos, S. T. Holmes, F. Mentink-Vigier, W. Zhang, Z. Du, C. Wu, M. J. Swamynadhan, Q. Zhao, K. Ye, D. A. Walko, N. S. Settineri, S. J. Teat, L. Zhao, R. W. Schurko, H. Wen, R. Mishra, and J. Ravichandran, Emergent atomic-scale polarization vortices, *Advanced Materials* **36**, 2311559 (2024).
- [35] P. Ranga, S. B. Cho, R. Mishra, and S. Krishnamoorthy, Highly tunable, polarization-engineered two-dimensional electron gas in ϵ - $\text{Al}_2\text{O}_3/\epsilon$ - Ga_2O_3 heterostructures, *Applied Physics Express* **13**, 061009 (2020).
- [36] P. He, M. Zhang, Y.-X. Huang, J. Li, R. Wang, S. Zhao, C. Pan, Y. Gao, T. Taniguchi, K. Watanabe, J. Hu, Y. Zhu, C. Xiao, X. C. Xie, S. A. Yang, and J. Shen, Giant field-tunable nonlinear hall effect by lorentz skew scattering in a graphene moire superlattice (2025), arXiv:2511.03381 [cond-mat.mes-hall].
- [37] V. M. Fridkin and B. N. Popov, Anomalous photovoltaic effect in ferroelectrics, *Soviet Physics Uspekhi* **21**, 981 (1978).
- [38] B. I. Sturman, Collision integral for elastic scattering of electrons and phonons, *Soviet Physics Uspekhi* **27**, 881 (1984).
- [39] S. Kryhin and L. Levitov, Collinear scattering and long-lived excitations in two-dimensional electron fluids, *Phys. Rev. B* **107**, L201404 (2023).
- [40] S. Kryhin, Q. Hong, and L. Levitov, Linear-temperature conductance in two-dimensional electron fluids, *Phys. Rev. B* **111**, L081403 (2025).
- [41] K. G. Nazaryan and L. Levitov, Nonlocal conductivity, continued fractions, and current vortices in electron fluids, *Phys. Rev. B* **110**, 045147 (2024).
- [42] J. Duan, Y. Jian, Y. Gao, H. Peng, J. Zhong, Q. Feng, and Y. Yao, Giant second-order nonlinearity in twisted bilayer graphene (2022), arXiv:2201.09274 [cond-mat.mes-hall].
- [43] Y. Kuramoto, Electronic higher multipoles in solids, *Progress of Theoretical Physics Supplement* **176**, 77 (2008).
- [44] Y. Kuramoto, H. Kusunose, and A. Kiss, Multipole orders and fluctuations in strongly correlated electron sys-

- tems, Journal of the Physical Society of Japan **78**, 072001 (2009).
- [45] P. Santini, S. Carretta, G. Amoretti, R. Caciuffo, N. Magnani, and G. H. Lander, Multipolar interactions in *f*-electron systems: The paradigm of actinide dioxides, Rev. Mod. Phys. **81**, 807 (2009).
- [46] V. A. Zenin, C. E. Garcia-Ortiz, A. B. Evlyukhin, Y. Yang, R. Malureanu, S. M. Novikov, V. Coello, B. N. Chichkov, S. I. Bozhevolnyi, A. V. Lavrinenko, and N. A. Mortensen, Engineering nanoparticles with pure high-order multipole scattering, ACS Photonics **7**, 1067 (2020).